



EVALUATION OF EARTHQUAKE INPUT ENERGY DISTRIBUTION IN AN RC BUILDING FOR AN ENERGY-BASED SEISMIC DESIGN APPROACH

Z. T. Deger ⁽¹⁾, F. Sutcu ⁽²⁾

⁽¹⁾ Inst.Dr., Istanbul Technical University, Earthquake Engineering and Disaster Management Institute, tunaz@itu.edu.tr

⁽²⁾ Assistant Professor, Istanbul Technical University, Earthquake Engineering and Disaster Management Institute, fatih.sutcu@itu.edu.tr

Abstract

Current seismic design codes of buildings are based on acceleration spectra in order to evaluate strength capacity which does not directly account for the influence of the duration of ground motion or the hysteretic behavior characteristic of the building. An energy-based approach to seismic design serves as an alternative index to response quantities like strength or deformation to include the duration-related seismic damage effects. Therefore, energy-based seismic design methodology is an alternative tool for the overall performance analysis of buildings.

Once the concept of input energy distribution is well-understood, energy dissipation capacity of moment resisting frames can be increased by providing special detailing in reinforced concrete buildings.

This paper aims to examine influences of ground motion characteristics and structural properties on distribution of input energy based on a four-story RC moment resisting frame building using different types of ground motions. For developing an energy-based design approach and assessing damage potential of buildings, distribution of earthquake input energy among energy components: kinetic, elastic strain, hysteretic, and structural damping has been investigated. Based on nonlinear analysis results, distribution of the earthquake-induced energy among floor levels as well as among structural components has been evaluated.

Keywords: Energy Based Design; Energy Components; Earthquake Input Energy; Structural Damping

1. Introduction

In current seismic design codes worldwide, the seismic structural design of buildings primarily rely on the strength and displacement capabilities of the structural members, such as ASCE/SEI 7-10 [1], Eurocode 8 [2], and Turkish Earthquake Code [3]. The maximum inter-story displacement is the structural response parameter most used for evaluating the inelastic performance of structures. However, it is well-known that the level of structural seismic damage does not depend only on maximum displacement. Fajfar *et.al.* has shown that the cumulative damage is a result of numerous inelastic cycles during a ground motion [4].

When a structure enters the inelastic range, deterioration of the hysteretic behavior occurs which can lead to failure of critical elements at deformation levels even below the ultimate deformation capacity of the structure. This damage is majorly affected by duration and called as cumulative damage, while this failure mode is called as low-cycle fatigue. However, most current design methods do not consider effects of low-cycle fatigue. Cumulative damage is commonly related to dissipated hysteretic energy which is a structural response parameter that provides a good evaluation basis for the plastic deformation and damage.

In current practice energy has not been used in the evaluation of the earthquake effects on structures and structural members in specific. Nevertheless, energy concept seems to have a great potential in the analysis of seismic demands and for the design of the structural members since energy approach implements strength and displacement characteristics of the structure together.

The Energy Based Seismic Design (EBS) subject was initially discussed by Housner [5]. Since then, many researchers have used the energy based design approach for the seismic analysis and structural design. In energy based design approach the first step is to evaluate the input energy that is induced by the ground motion to the structure. Akiyama [6] proposed a three-step method to obtain the design energy input spectrum for a given region from the individual energy input spectra obtained for each available ground motion record. Later, Decanini *et.al.* [7] Benavent-Climent *et.al.* [8,9] constructed design energy input spectra applicable to the seismic design of structures by using ground motions recorded in specific regions and improving the parameters considered such as soil properties or ground motion intensity. However, in this study, the design input energy will not be discussed and the main topic is the dissipation of earthquake induced energy through structural components.

This paper aims to examine the distribution of input energy based on a four-story RC moment resisting frame building. For developing an energy-based design approach and assessing damage potential of buildings, distribution of earthquake input energy among energy components: kinetic, elastic strain, hysteretic, and structural damping has been investigated. Based on nonlinear analysis results, distribution of the earthquake-induced energy among floor levels as well as among structural components has been evaluated.

2. Components of Energy Balance

The equation of motion for a SDOF system subjected to a ground motion is given by the following equation:

$$m\ddot{y} + c\dot{y} + Q(y) = -m\ddot{y}_g \quad (1)$$

In Eq. (1) m is the mass, c is the damping coefficient, $Q(y)$ is the restoring force, y is the relative displacement to the ground, and \ddot{y}_g is the ground acceleration. Multiplying Eq. (1) by $dy = \dot{y}dt$ and integrating along the duration of the earthquake gives

$$\int_0^t m \ddot{y} \dot{y} dt + \int_0^t c \dot{y} \dot{y} dt + \int_0^t Q(y) \dot{y} dt = - \int_0^t m \ddot{y}_g \dot{y} dt \quad (2)$$

In Equation 2 the terms on the left hand side represent the energy components of the structure. The first, second, and third terms are relative kinetic energy (E_K), structural energy dissipated by inherent damping (E_D), and absorbed energy (E_A), respectively. The right-hand side of the equation represents the total input energy (E_I) that is induced to the structure by the earthquake. If the equation is re-arranged:

$$E_K + E_D + E_A = E_I \quad (3)$$

The absorbed energy E_A consists of recoverable elastic strain energy, E_{ES} and irrecoverable hysteretic energy, E_H where $E_{ES} = Q(y)^2/2k$ and $E_H = E_A - E_{ES}$, in which k is the initial stiffness of the structure. Kinetic energy, E_K is also recoverable and the sum of E_{ES} and E_K gives the elastic vibrational energy E_E , then Eq. 3 can be re-written as:

$$E_E + E_D + E_H = E_I \quad (4)$$

The elastic vibrational energy E_E diminish at the end of the ground motion, whereas the damping and hysteretic energies are dissipated by the structure during the ground motion. It is obvious that, the duration of strong motion significantly affects the maximum damping energy, the maximum hysteretic energy, and the maximum input energies, but not the maximum kinetic energy and the maximum elastic strain energy.

The dissipated energies are critical in the evaluation and design of the structures by using energy-based design approaches. Structural damage should be limited by providing sufficient ductility and energy dissipation capacity by hysteretic action and/or damping in the structure. The damage potential is related with the total hysteretic energy demand during the excitation. The hysteretic energy demand can be computed from the input energy spectra if the ratio of the hysteretic energy to the input energy is known. Some studies suggest that there is a consistent relation between the input and hysteretic energies [10-12].

In this study, consistency of the relations between energy components is investigated through non-linear response history analyses on a four-story reinforced concrete moment frame building. Based on computer-based nonlinear analysis results, distribution of the earthquake-induced energy among floor levels as well as among structural components has been evaluated. The analytical model was created based on a full-scale specimen tested in E-Defense shaking table facility in late 2010. Analysis results are compared to the experimental results for verification of the analytical model and test results.

3. Description of the E-Defense Tests

Two full scale, four story buildings were tested simultaneously by the National Research Institute for Earth Science and Disaster Prevention (NIED) at the E-Defense shake table facility in Miki, Japan in December 2010. One building was designed as a conventional reinforced concrete building, whereas the other building was a high-performance post-tensioned building. Total weight of each building was approximately 602.4 tons (including the base), thus, two buildings together utilized almost full capacity of the E-Defense shake table. The test buildings were subjected to increasing intensity shaking using the 1995 Kobe earthquake ground motions recorded at JMA-Kobe and JR-Takatori stations until near collapse state was reached. The testing sequence was 25%, 50%, and 100% JMA-Kobe motions followed by 40% and 60% Takatori motions.

Fig.1 presents pseudo acceleration, pseudo velocity, and displacement spectra as well as spectra for a service level (SLE; 50% in 30 years), design level (DBE; 10% in 50 years), and maximum considered earthquake level (MCE; 2% in 50 years) based on ASCE 7-10 requirements [13] assuming that the buildings were located in downtown Los Angeles for Site Class B. Peak spectral accelerations observed on the shaking table were 0.58g, 1.18g and 2.79g at 25%, 50% and 100% Kobe records, respectively. Comparisons of spectral demands with

code-specified spectra at the fundamental period of the building (approximately 0.4 sec in the frame direction) revealed that demands for the 25% and 50% Kobe records were close to the SLE and DBE spectra, respectively, whereas demands for the 100% Kobe record were much higher than the MCE spectrum.

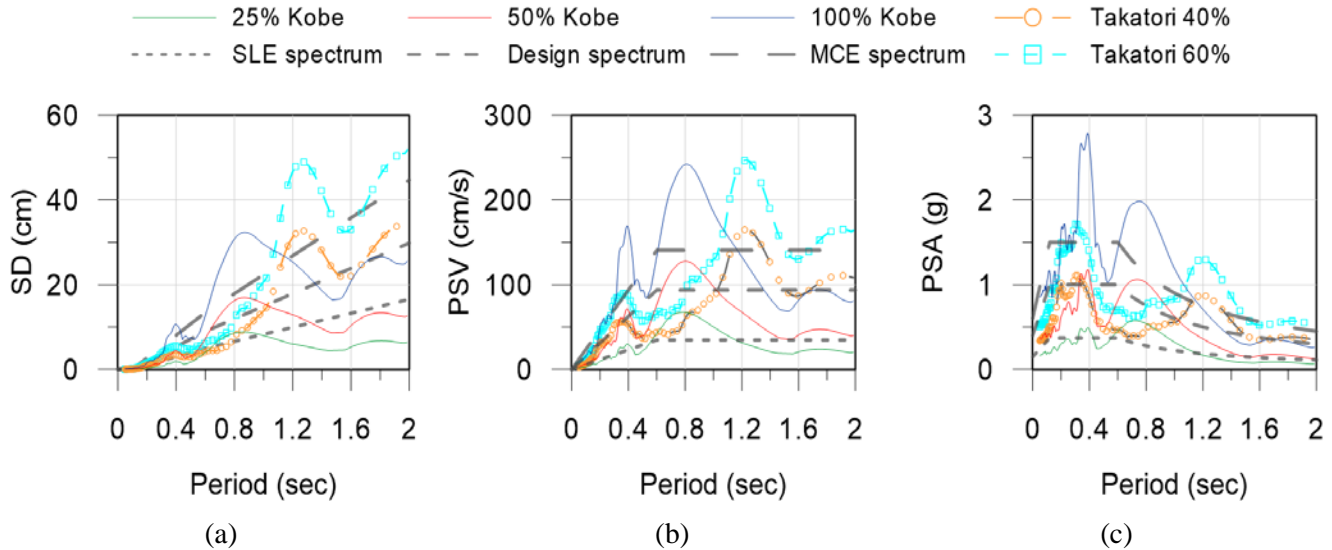


Fig.1 – (a) Displacement spectra, (b) pseudo-velocity spectra, (c) pseudo-acceleration spectra

From the above-mentioned two test specimens, conventional reinforced concrete building (RC) was used as the basis of this study. The building had floor dimensions of 14.4 m x 7.2 m and story height of 3 m, as shown in Fig.2. The building was designed using the latest code requirements in Japan ([14], [15]) and generally satisfied ACI 318-08 [16] and ASCE 7-05 [13] requirements with an exception of strong column-weak beam requirements. Lateral load resisting system of the building was consisting of shear walls and moment frames in the short and long directions, respectively.

This paper concentrates on the two-bay frame direction of the building where 500mm x 500 mm columns were connected by 300mm x 600 mm beams. Axial load levels were $0.12A_g f'_c$ and $0.06A_g f'_c$ for the interior (C2) and exterior (C1) columns, respectively. Exterior columns had longitudinal reinforcement of 10-D22 bars and 8-D22 bars for the first floor and upper floors, respectively, whereas interior columns included 10-D22 bars at all floors. Design concrete strength was specified as $f'_c=27$ MPa whereas as-tested material properties were reported as 39.6 MPa, 39.2 MPa, 30.2 MPa and 41.0 MPa for first, second, third, and fourth floor, respectively [17], i.e., approximately 1.4 times the design value. As tested reinforcing steel yield strength was reported as $f_y=370$ MPa for 22-mm diameter bars, which was about 1.1 times the design value.

Example test results are presented in Fig.3 for the Kobe records. Peak roof displacements (Fig.3 (a)) were 1.86 cm, 12.88 cm, and 25.36 cm with corresponding roof drifts of 0.16%, 1.07%, and 2.11% at 25%, 50%, and 100% Kobe records, respectively. Residual roof displacement of 7 cm (0.6% drift) was noted for the 100% Kobe record. Base shear versus roof drifts were plotted in Fig.3(b), where base shear was calculated by multiplying floor masses by absolute floor accelerations. Experimental results indicate that the building remained elastic at the 25% Kobe record, whereas modest inelastic response associated with yielding was observed at the 50% Kobe record. Significant yielding and stiffness degradation were noted for the 100% Kobe record.

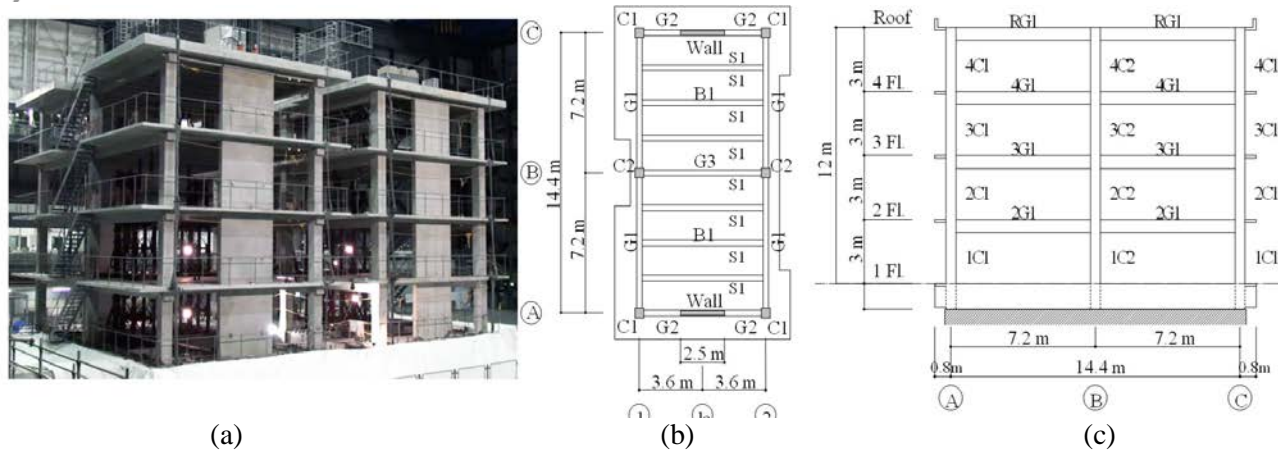


Fig.2 – a) View from the experiment, b) plan view of the RC Building, c) elevation view of the RC Building

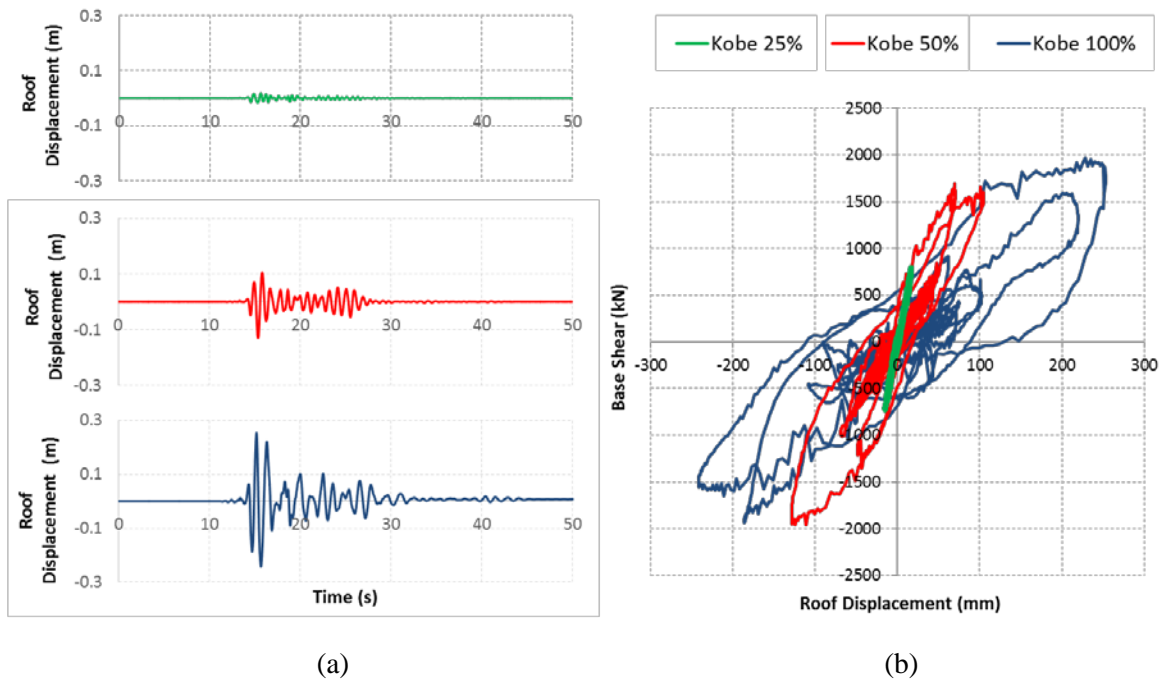


Fig.3 – Experimental results: (a) roof displacement histories, (b) base shear versus roof displacement relations

4. Analytical Modeling

Nonlinear analytical model of the reinforced concrete building was developed in the frame direction (axes 1 and 2 in Fig.2) using structural analysis software CSI Perform 3D[18]. Frame members were modeled based on lumped plasticity assumption using elastic elements with plastic hinges and rigid end zones. Elastic portion of beams and columns were modeled such that gross section properties and cracked section properties with effective stiffness of $EI_{eff} = 0.2EI_g$ (based on section analysis) were used up to cracking moment and after cracking moment, respectively. It is noted that parallel stiffness element was used to achieve this behavior and stiffness was dropped to zero after cracking moment is reached. Beam cross-sections were modeled including effective slab width based on ASCE 41-13 [19]. Plastic hinges were consisting of P-M interaction curves and moment-rotations relations for columns and beams, respectively. Beam moment-rotation hinges were defined as elastic-perfectly plastic including cyclic degradation and strength loss based on ASCE 41-13 [19] modeling

criteria. Floor masses were lumped at column nodes. Foundation was assumed as fixed-base. Rigid diaphragm was assigned at each floor. P-Delta effects are included in the analysis.

Damping of the building was modeled by the Rayleigh damping, i.e. mass and stiffness proportional damping in a linear combination. Constants α and β of the mass and initial stiffness matrices, respectively, were calculated automatically by the software such that the critical damping ratio was 5% at $0.2T_1$ and T_1 where T_1 is the fundamental period [20]. It is noted that results were not sensitive to the damping parameters selected. Ground (shake-table) motions were applied in the same sequence as the experiment to reflect the actual testing, i.e., the sequence was: 25% Kobe + 50% Kobe + 100% Kobe.

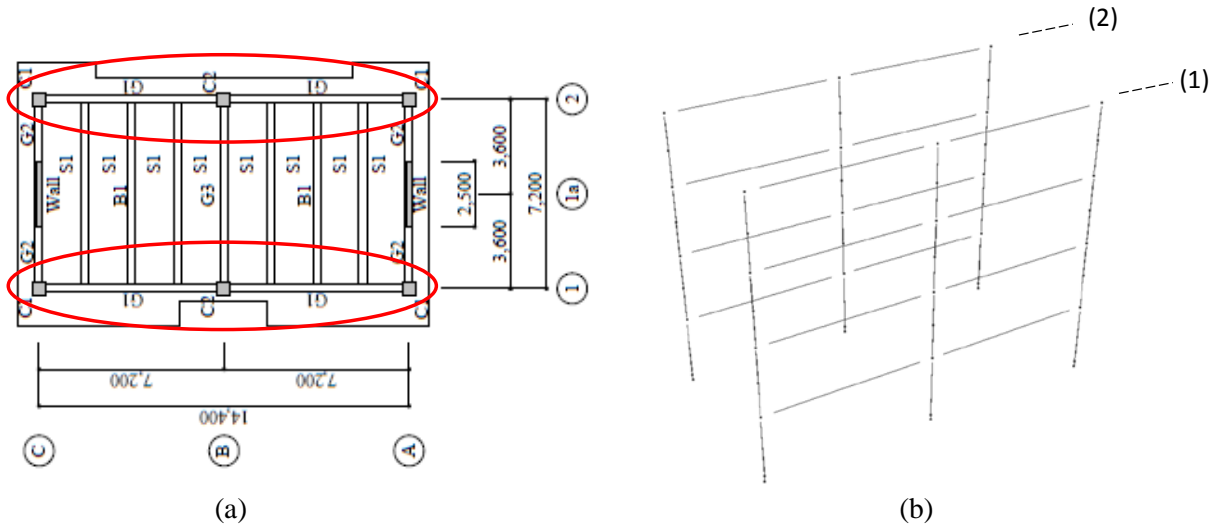


Fig. 4 – a) Plan view of the building model, b) isotropic view of the model in Perform 3D

Fig.5 shows that analysis results were consistent with test results at 25% and 50% Kobe records, where overall stiffness and peak displacements were captured. Peak displacements and stiffness degradation are underestimated at 100% Kobe record although base shear was well estimated. Residual displacement was overestimated (in the negative direction) at 100% Kobe record (Fig.5(c)). Potential reasons for the discrepancies observed at 100% Kobe record may be (i) neglecting the change in column effective stiffness due to variation of axial demands, (ii) underestimating stiffness reduction due to slip/extension deformations at beam and column-joint interfaces [21], (iii) cyclic degradation parameters selected in the analytical model. It is noted that use of fiber elements (versus elastic elements with plastic hinges) may help reducing the inconsistencies between the experimental and analytical results, which will be considered in future studies.

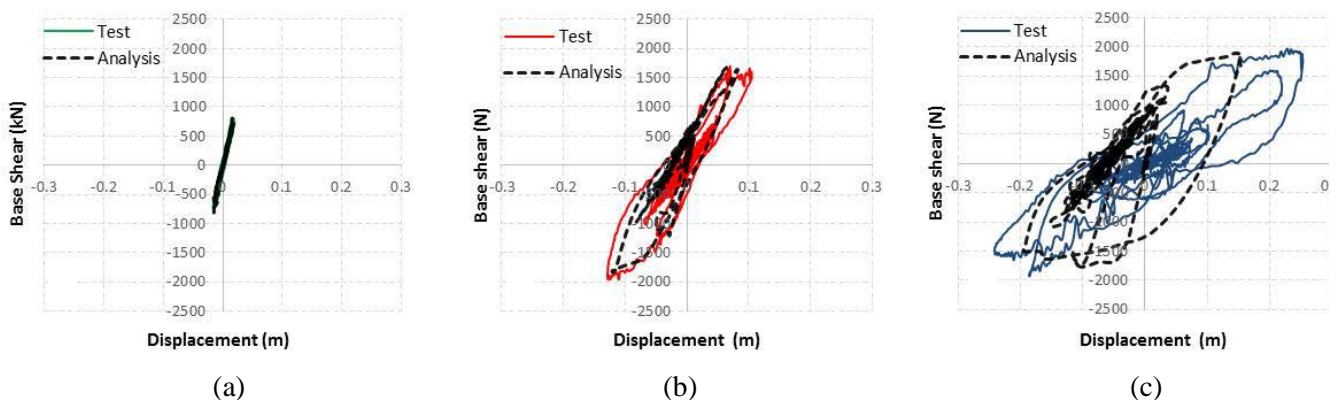


Fig.5 – Comparisons of test and analytical results at a) 25% Kobe, b) 50% Kobe, and c) 100% Kobe records

5. Energy Response

Although some discrepancies were observed between analytical and experimental results of the four-story RC frame building tested at E-Defense, the model was found to be sufficiently representative of the test building as responses were reasonably captured. Therefore, the model was used to assess components of earthquake-induced energy as well as energy distribution within the structural elements and stories of the building.

Energy components along with their percentage to the total energy are presented in Fig.6 for 25%, 50%, and 100% Kobe records. Total input energy E_I consists of kinetic energy (E_K), elastic strain energy (E_{ES}), structural damping (α -M and β -K) energies (E_D), and hysteretic or dissipated inelastic energy (E_H); the first two of which diminish to zero by the end of the ground motion record as explained by Eq.3 and Eq. 4. Total hysteretic energy was calculated as 0.03 kN-m, 39 kN-m, and 404 kN-m for 25%, 50%, and 100% Kobe records, respectively. At 25% Kobe record, hysteretic energy was not observed as the structure remained elastic due to the low level of input intensity, relatively short ground motion relation and as a result, low levels of input energy; therefore, almost the entire energy was dissipated by structural damping mechanism. At higher levels of excitation, i.e., larger earthquake-induced input energy in the structure, approximately 15% and 30% of the total energy at 50% and 100% Kobe records, respectively, was due to inelastic deformations, i.e., dissipated as hysteretic energy, E_H .

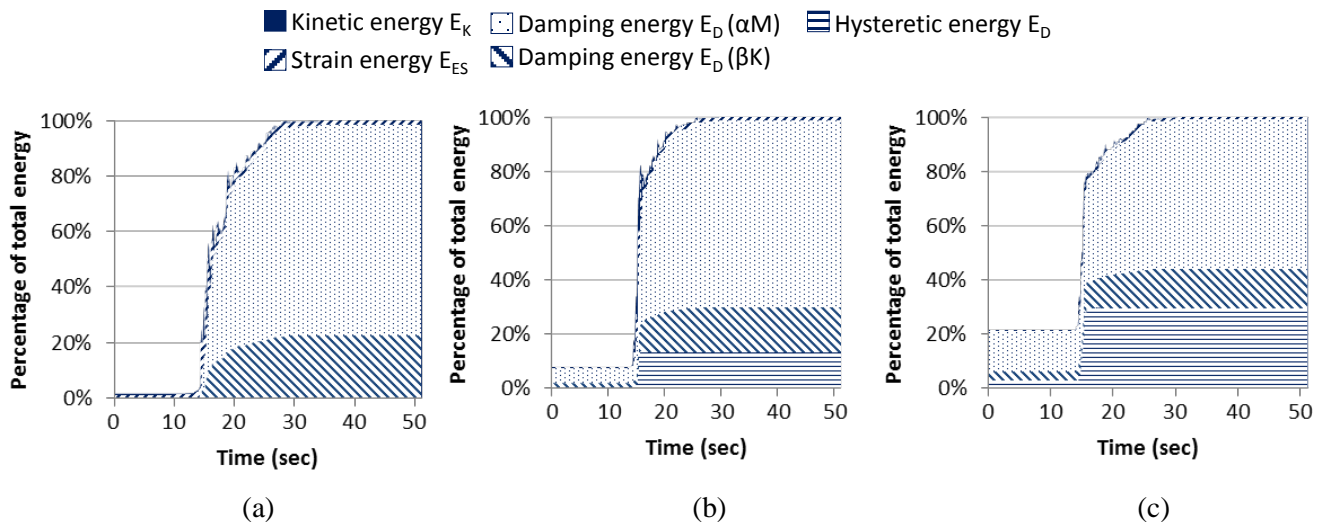


Fig.6 – Energy distribution at a) 25% Kobe, b) 50% Kobe, c) 100% Kobe records

Distribution of dissipated inelastic (hysteretic) energy, E_H among structural elements was also investigated based on nonlinear response history analyses for 50% and 100% Kobe records. Energy distribution among floors is presented in Fig.7, whereas more detailed distribution among structural elements are summarized in Table 1. Consistent with the damage observed in the building, largest fraction of the hysteretic energy was dissipated in first floor columns (about 50% of the total hysteretic energy), followed by first floor beams (about 30% of the total hysteretic energy). Results revealed that energy distribution among stories was not sensitive to ground motion intensity.

Table 1 – Distribution of hysteretic energy among structural elements

Element group	50% Kobe record	100% Kobe record
Columns – Floor 1	50.3%	46.3%
Columns – Floor 2	2.3%	4.2%
Columns – Floor 3	2.0%	0.9%
Columns – Floor 4	0.0%	0.6%
Beams – Floor 1	30.8%	32.4%
Beams – Floor 2	14.4%	14.3%
Beams – Floor 3	0.0%	1.0%
Beams – Floor 4	0.0%	0.0%

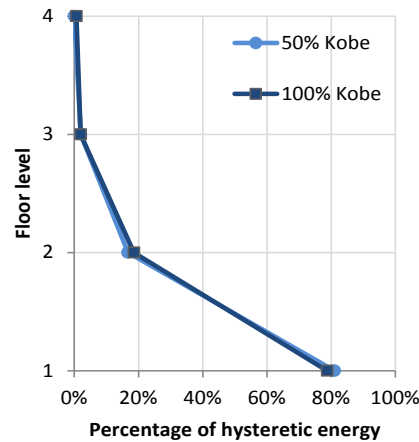


Fig.7 – Distribution of hysteretic energy among floor levels

Response history analyses were repeated using other ground motion records to investigate effects of earthquake motion characteristics on the distribution of energy components in the building. The following ground motion records with properties shown in Table 2 were scaled and applied to the model individually after gravity loading: El Centro (1940), Duzce (1999), and Cape Mendocino (1992).

Table 2 – Ground Motion Record Properties

Ground Motion Record	PGA (g)	PGV (cm/s)	Arias Intensity (m/s)	Scaling Factor	Effective duration D5-95(s)
	Unscaled/Scaled				
El Centro (1940)	0.254/0.381	31.03/46.54	1.6/2.4	1.5	24.2
Duzce (1999)	0.515/0.515	84.27/84.27	2.9/2.9	1.0	11.1
Cape Mendocino (1992)	1.494/1.792	122.63/147.16	6/7.2	1.2	9.7

To allow consistency, El Centro, Duzce, and Cape Mendocino records were scaled by a factor of 1.5, 1.0, and 1.2, respectively, such that input energy of each of ground motion was similar (approximately 470 kN-m). Base shear versus roof displacement relations obtained from each analysis is shown on Fig.8 and energy components along with their percentage to the cumulative energy are presented in Fig.9.

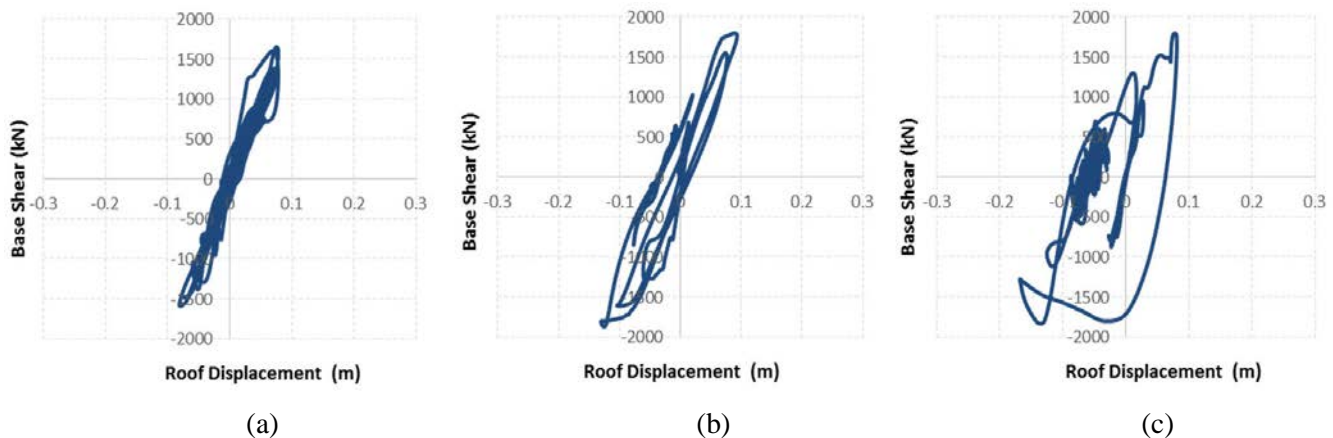


Fig.8 –Base shear versus roof displacement relations for a) El Centro, b) Duzce, c) Cape Mendocino

Percentage of dissipated hysteretic energy (E_H) for El Centro, Duzce, and Cape Mendocino records were obtained as 3%, 20%, and 25%, respectively, as shown on Fig. 9. It is observed that E_H percentage for El Centro record was significantly low compared to the other two records. As the total input energy levels were scaled and made comparable for the three ground motions, low level of hysteretic energy component for El Centro record shows that the building essentially remained elastic and major part of the energy was dissipated through structural damping mechanism. This behavior can be clearly seen in Fig 8(a).

Earthquake induced hysteretic energy is basically derived from strength and structural dynamic response integrated over earthquake duration. Percentage of energy components obtained from El Centro record corroborates this statement, as same amount of input energy was induced in the model within a longer duration and lower acceleration intensity compared to other records. Comparison of Duzce and Cape Mendocino analysis results revealed that hysteretic energy component E_H obtained from the latter record was higher, due to higher intensity, even though the effective durations were similar.

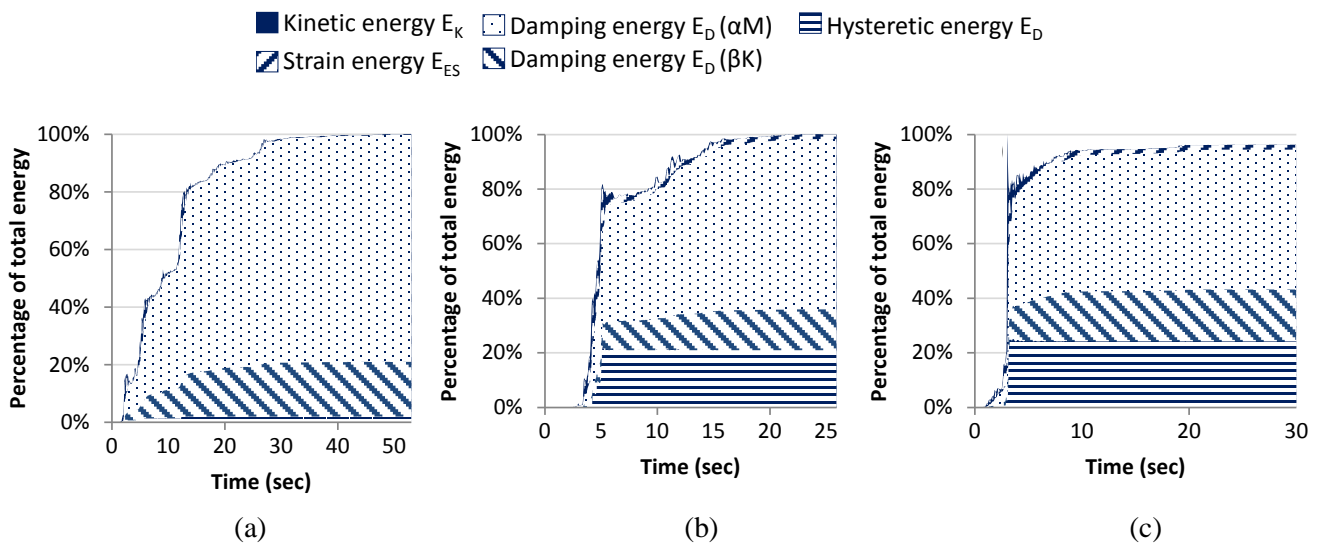


Fig.9 – Energy distribution at a) El Centro, b) Duzce, c) Cape Mendocino records

6. Conclusions

Effects of ground motion characteristics on distribution of input energy components were investigated based on a four-story reinforced concrete moment resisting frame building using different types of ground motions. To develop an energy-based design approach and to assess damage potential of existing buildings, distribution of earthquake input energy among energy components, namely: kinetic, elastic strain, hysteretic, and structural damping stands for great importance. Nonlinear analytical model of the four-story, full-scale RC building tested on the E-Defense shake table was built in CSI Perform 3D and calibrated based on the experimental results. Based on nonlinear analysis results, distribution of the earthquake-induced energy among floor levels as well as among structural components have been assessed for a variety of ground motion records with different seismic characteristics. Results have shown that input intensity has no significant influence on the distribution of energy components.

Input energy and energy components are highly affected by the duration of the ground motion and structural responses such as response velocity and displacement. Comparison of energy responses for different ground motion records has shown that increasing effective duration or ground motion intensity increases the hysteretic energy component which is essentially related to structural damage. Future studies will include further investigating the relation between effective duration, input intensity, and energy components through comprehensive parametric and analytical studies.

7. References

- [1] ASCE/SEI 7-10 (2010), Standard, American Society of Civil Engineers (ASCE), Minimum Design Loads for Buildings and Other Structures, Reston, VA.
- [2] Eurocode 8, (2004), European Committee for Standardization Design of Structures for Earthquake Resistance, B-1050, Brussels.
- [3] Turkish Earthquake Code (TEC), 2007. Specification for Structures to be Built in Disaster Areas, Ministry of Public Works and Settlement, Government of the Republic of Turkey, Ankara.
- [4] Fajfar P, Vidic T. (1994) Consistent inelastic design spectra: hysteretic and input energy. *Earthquake Engineering and Structural Dynamics*; 23:523–37.
- [5] Housner, G. W., (1956). Limit Design of Structures to Resist Earthquakes, *Proceedings of First World Conference on Earthquake Engineering*, Berkeley, CA, 1–13.
- [6] Akiyama, H., (1985). Earthquake-Resistant Limit-State Design for Buildings, University of Tokyo Press.
- [7] Decanini L.D. and Mollaioli, F. (1998). Formulation of elastic earthquake input energy spectra. *Earthquake Engineering and Structural Dynamics* **27**, 1503-1522.
- [8] Benavent-Climent, A., Pujades, L.G. and Lopez-Almansa, F. (2002). Design energy input spectra for moderate seismicity regions. *Earthquake Engineering and Structural Dynamics* **31**, 1151-1172.
- [9] Benavent-Climent, A., Lopez-Almansa, F. and Bravo-Gonzales, D. A. (2010). Design energy input spectra for moderate-to-high seismicity regions based on Colombian earthquakes. *Soil Dynamics and Earthquake Engineering* 30 1129–1148
- [10] Decanini, L. D., and Mollaioli, F., 2001. An energy-based methodology for the assessment of seismic demand, *Soil Dynamic and Earthquake Engineering* 21, 113–137.
- [11] Manfredi, G., 2001. Evaluation of seismic energy demand, *Earthquake Engineering and Structural Dynamics* 30, 485–499.
- [12] Lopez-Almansa, F., Yazgan, A. U., and Benavent-Climent, A., 2013. Design energy input spectra for high seismicity regions based on Turkish registers, *Bulletin of Earthquake Engineering* 11, 885–912.
- [13] ASCE/SEI 7. (2010). Minimum Design Loads for Buildings and Other Structures, Structural Engineering Institute of the American Society of Civil Engineers.
- [14] AIJ, Design Guidelines for Earthquake Resistant Reinforced Concrete Buildings Based on the Inelastic Displacement Concept, Architectural Institute of Japan, Tokyo, Japan, 440 pp, 1999. (in Japanese)
- [15] MLIT, Technological Standard Related to Structures of Buildings, Ministry of Land, Infrastructure, Transport, and Tourism, Tokyo, Japan, 2007.
- [16] ACI 318-08, 2008. “Building Code Requirements for Structural Concrete and Commentary,” American Concrete Institute Committee 318.
- [17] Nagae, T.; Wallace, J. W., 2011. Design and instrumentation of the 2010 E-Defense four-story reinforced concrete and post-tensioned concrete buildings, PEER Report, PEER-2011/104. June 2011, UC Berkeley.
- [18] CSI Perform 3D V5, 2011. Nonlinear Analysis and Performance Assessment for 3D Structures, Computer and Structures, Inc. Berkeley, CA.
- [19] ASCE/SEI Seismic Rehabilitation Standards Committee, 2007. Seismic Rehabilitation of Existing Buildings (ASCE/SEI 41-06), American Society of Civil Engineers, Reston, VA, US.
- [20] Applied Technology Council, 2010. ATC-72: Modeling and Acceptance Criteria for Seismic Design and Analysis of Tall Buildings. ATC, Redwood City, CA.
- [21] Elwood, K. J., Matamoros, A. B., Wallace, J. W., Lehman, D. E., Heintz, J. A., Mitchell, A. D., Moore, M. A., Valley, M. T., Lowes, L. N., Comartin, C. D., and Moehle, J. P., 2007. Update to ASCE/SEI 41 Concrete Provisions. *Earthquake Spectra*, Vol. 23, No. 3, pp. 493-523.